analytical chemistry

Letter

pubs.acs.org/ac

High Lateral Resolution vs Molecular Preservation in near-IR fs-Laser Desorption Postionization Mass Spectrometry

Yang Cui, Igor V. Veryovkin, Michael W. Majeski, Daniel R. Cavazos, and Luke Hanley*

Department of Chemistry, University of Illinois at Chicago, MC 111, Chicago, Illinois 60607, United States

Supporting Information

ABSTRACT: Ultrashort pulse length lasers operating in the near-infrared region show promise for submicrometer lateral resolution by laser desorption-based mass spectrometry (MS) imaging. However, these experiments must balance lateral resolution and molecular fragmentation since abundant atomic ions are observed at the high laser irradiances that can be generated by tightly focused ultrashort pulse laser beams. It is shown here that combining ultrashort pulse laser desorption with laser postionization (fs-LDPI) allows for a considerable increase of molecular ion signal while operating with lower laser irradiances, yielding the added benefit of reduced molecular fragmentation. This Letter presents several experimental results in support of the fs-LDPI approach for MS imaging. First, the lateral resolution for MS imaging of molecular species desorbed by ~75 fs, 800 nm laser pulses was determined to be <2 μm for a simulated organic electronic device under vacuum. Next, the dependence of precursor ion survival on both desorption laser fluence and delay between desorption and photoionization laser pulses was observed for a small molecule desorbed from an organic multilayer that was originally devised as a model of a bacterial biofilm. When considered in light of recent results in the literature (Milasinovic et al. *J. Phys. Chem. C* **2014**, DOI: 10.1021/jp504062u), these experiments demonstrate the potential for submicrometer spatial resolution MS imaging by fs-LDPI.

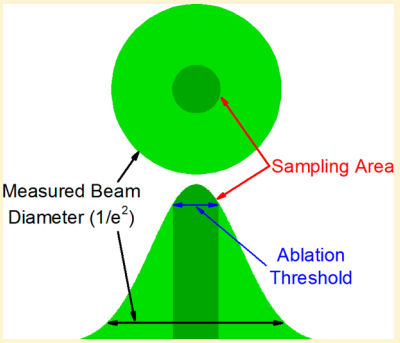

Laser desorption (LD)-based mass spectrometry (MS) imaging is under intense study for spatially resolved molecular analysis of intact biological samples, biomaterials interfaces, and electronic devices.[1−6] Matrix assisted laser desorption ionization (MALDI) with ultraviolet (UV) lasers is the premier LD-based method in MS imaging capable of preserving molecular structure with typical lateral resolutions approaching ~25 μm.[6] Lateral resolution approaching 5 μm has been achieved in MALDI using high numerical aperture optics,[7] aspheric optics with Gaussian laser beams,[8] imaging in microscope mode,[9] and back of sample irradiation of thin slices.[10] Near field optical strategies have also been examined for this goal.[11] However, MS imaging of single cells and other submicrometer sized structures require lateral resolution beyond 5 μm that remains elusive by MALDI specifically[6,12] and LD generally.[5] Secondary ion mass spectrometry can achieve submicrometer spatial resolution[1,2] but so far only with primary ion sources that tend to enhance molecular fragmentation.[13,14]

Ultrashort pulse length lasers operating in the near-infrared (IR) region show promise for LD-based MS imaging.[5,15,16] The most common configuration operates using a Ti:sapphire laser to create ~75 fs, 800 nm pulses which can generate useful molecular ion signal without addition of a matrix. Recent experiments have shown that fs-LD can enable internal energy transfer in vacuum[17] or at atmospheric pressure[18] comparable to that of MALDI performed at the corresponding background pressure. Near-IR fs laser pulses can be used to directly desorb either precursor ions[15,17] or neutrals for postionization by vacuum UV (VUV) radiation[16,17] or electrospray.[18]

Near-IR fs-LD has previously demonstrated 10 to 30 μm lateral resolution MS imaging of intact plant leaves[15] and biofilms,[16] respectively. However, the optimum lateral resolution of fs-LD MS imaging should approach that of the submicrometer sized features that have been micromachined into biological and synthetic structures by ultrashort laser pulses.[19] One caveat to the submicrometer goal for fs-LD MS imaging is the balance between lateral resolution and molecular fragmentation since abundant atomic ions are observed at the high laser irradiances that can be generated by tightly focused fs-LD beams.[16,20,21] Combining fs-LD with laser postionization (fs-LDPI) allows for a considerable increase of molecular ion signal while operating with lower laser irradiances, yielding the added benefit of reduced molecular fragmentation.[16,17] For such cases, especially when desorption is performed under vacuum, the time delay between the fs-LD and postionization laser pulses becomes an important factor influencing the extent of molecular fragmentation.

This Letter presents several experimental results in support of the fs-LDPI approach for high lateral resolution MS imaging. First, the lateral resolution for MS imaging of molecular species by ~75 fs, 800 nm pulsed LD is determined here for a

Received: November 4, 2014
Accepted: December 4, 2014
Published: December 4, 2014

simulated organic electronic device under vacuum.[16,20] Next, the dependence of precursor ion survival on both desorption laser fluence and delay between desorption and photoionization laser pulses is observed for a small molecule desorbed from an organic multilayer (originally devised as a model of a bacterial biofilm).[17,22] When considered in light of recent results in the literature,[17] these experiments demonstrate the potential for high lateral resolution MS imaging by fs-LDPI.

EXPERIMENTAL DETAILS

Experiments were performed with a home-built laser desorption postionization reflectron time-of-flight mass spectrometer[16,20] operating in microprobe mode using ~75 fs, 800 nm, nominally p-polarized laser pulses from a Ti:sapphire laser for fs-LD of samples under vacuum of $\sim 10^{-7}$ mBar. Photoions were formed by 10.5 eV VUV (~8 ns, 118 nm) single photon ionization of gaseous neutrals formed by fs-LD.[16] The repetition rate of the overall fs-LDPI-MS measurement was limited to 10 Hz by the Nd:YAG laser pumping a Xe/Ar cell, where the 355 nm third harmonic output was frequency tripled to produce 10.5 eV VUV photons.[16,23] For imaging, a computer controlled in-vacuum *XYZ* translation stage was used to raster scan the sample with submicrometer precision as observed by an integrated optical microscope.[20] An objective (NA 0.28, Mitutoyo, Japan) was used to focus the desorption laser beam for imaging experiments at the highest spatial resolution while an achromatic double lens (200 mm focal length, Thorlabs, NJ, US) was used for nonimaging experiments at optimal signal-to-noise ratio. An experimental diagram and further details of the fs-LDPI-MS instrument are provided in the Supporting Information.

Two types of samples were prepared for these measurements. First, micrometer-scale square patterns of pentacene (P0030, TCI of America, Portland, OR, USA) were deposited onto an underlying Si wafer by sublimation from a heated ceramic crucible (LTE 11000K, 1 cc, Kurt J. Lesker, Pittsburgh, PA, USA) at 160−190 °C through an electron microscopy grid (16.5 μm pitch: 11.5 μm hole width and 5 μm bar width, G1500HS, SPI, West Chester, PA). Second, polyelectrolyte multilayers composed of ten layers each of chitosan and alginate were adsorbed onto an Au-coated Si wafer[22] and then doped with a small molecule analyte, 2-methoxy-4-amino-5-chlorobenzoic acid (GMW 201.6).

RESULTS AND DISCUSSION

Figure 1 shows optical and MS images of pentacene deposited through an electron microscopy grid onto the Si wafer. The center of the optical image displays the region that was analyzed by fs-LDPI-MS, and depletion of the pentacene by fs-LD is clearly visible. The energy of the desorbing fs-laser was ~20 nJ/pulse, and the time delay between desorption and photoionization laser pulses was set to 25 μs in order to maximize ion signal. MS imaging was performed by moving the translation stage continuously at a rate of 5 μm/s along the *X*-axis, collecting two mass spectra per pixel, and by 1 μm steps along the *Y*-axis. The MS image was constructed from the signal for intact pentacene ions at m/z 278 ± 0.5 with an effective pixel size of 1 μm^2. The 16.5 μm grid pitch is marked on the MS image. An MS image line scan is also shown in Figure 1 for the integrated signal from the yellow shaded region of the MS image. The fs-LD probe size, corresponding to the lateral resolution, was estimated by extracting the 25−75% intensity

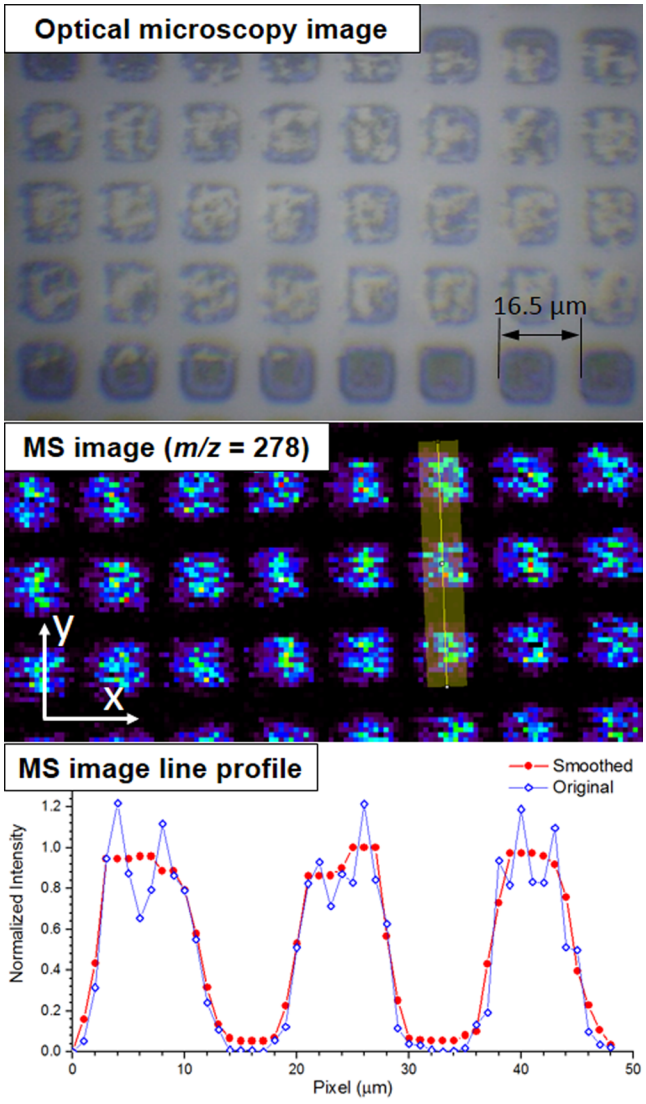

Figure 1. Micrometer-scale square pattern of pentacene deposited through an electron microscopy grid onto a Si wafer by sublimation from a heated ceramic crucible, imaged by the fs-LDPI-MS instrument (middle) and by an integrated optical microscope after MS analysis (top). Grid dimensions were: 16.5 μm pitch, 11.5 μm hole width, and 5 μm bar width. One MS image pixel corresponds to a 1 μm sample translation step. The line scan for the MS image area (obtained by signal integration of the yellow shaded region) demonstrates lateral resolution of ~2 μm (bottom). A percentile filter smoothing of the original data was used to determine the average signal level corresponding to 100% intensity for extracting and comparing 25−75% levels for estimating spatial resolution.

levels from the MS line scan by the established knife edge method[24] and yielded a <2 μm value, less than half of the ~4 μm diameter ($1/e^2$) of the 800 nm laser beam (see the Supporting Information).[25] VUV laser postionization allowed fs-LD to be recorded at lower laser fluences so that *desorption occurred from spots considerably smaller than the laser beam focal spot* (see TOC graphic and Supporting Information). This mode employs the phenomenon of nonlinear optical absorption, where only the intensity above a certain threshold is absorbed by the material leading to its explosive ablation.[26] This phenomenon is particularly pronounced in ultrashort laser pulse interactions with solids[26,27] where it has enabled

dx.doi.org/10.1021/ac5041154 | *Anal. Chem.* 2015, 87, 367−371

submicrometer lateral resolution of fs laser micromachining of inorganic,[28] organic, and biological material.[19,29−31]

However, use of this precision ablation in MS imaging is limited by the fact that low fluxes of desorbed/ablated material contain far fewer molecular and atomic species than are typically observed by LD-based MS instruments, drastically limiting the number of (even less abundant) ions available for mass analysis. For this reason, high lateral resolution fs-LD MS imaging was facilitated here by VUV single photon ionization of desorbed neutrals (fs-LDPI).[32] Prior results found higher sensitivities for the detection of photoions by fs-LDPI than direct ions by fs-LD for species desorbed from intact bovine eye tissue.[17] A crude estimate indicates that <1 femtomole of pentacene can be detected by this specific fs-LDPI-MS instrument, but additional study is required to more accurately determine the limit of detection.

It is important to recognize that the <2 μm resolution observed here is not a fundamental limit for the fs-LDPI technique because the specific MS instrument employed here suffered from excessive mechanical vibrations and suboptimal ion transmission. These factors collectively reduced instrumental sensitivity and prevented operation with the lower laser fluences required for higher lateral resolution. Other factors may have also degraded the spatial resolution, specifically the "fuzziness" of the pentacene pattern edges originating from the sample fabrication process.

Five μm size features on a patterned photoresist were previously distinguished by LD using the higher intensity central portion of a ∼30 μm diameter, UV ns pulse length laser beam (performed in the absence of added matrix).[33] However, UV ns-LD can induce photochemical reactions in samples even in the linear intensity (low irradiance) regime, which limits the ability of ns-LD to perform MS analyses of biological samples, unless matrix is added to facilitate MALDI. Photochemistry is deleterious because it can contribute to molecular fragmentation during MS imaging. It can be argued that these were some of the original motivations for the development of MALDI. In contrast, the possibility of laser-induced photochemical alteration of many microbial and fungal biofilms, most mammalian tissue, and many other biological samples is minimized by their transparency in the linear intensity regime for the 800 nm wavelength.[34] Experiments applying near-IR fs-LD MS with VUV postionization to the pentacene patterned sample revealed mass spectra with almost no ion fragments (see the Supporting Information), allowing the high signal-to-noise MS image shown in Figure 1 to be constructed entirely from the intact pentacene ion.

Recent experiments using fs-LDPI observed an increase in fragmentation of a thermometer molecule with increased overlap between adjacent laser spots, lower desorption laser fluence, and shorter delay time between the firing of the desorption and photoionization lasers.[17] In order to clarify the interplay between these parameters and molecular fragmentation, some of these issues were revisited here in nonimaging mode on a sample that approximates intact biological material, a chitosan−alginate polyelectrolyte multilayer onto which a metabolite analogue was adsorbed.[22] Figure 2 shows the fs-LDPI-MS of 2-methoxy-4-amino-5-chlorobenzoic acid desorbed from the multilayer at laser pulse energies of 0.11, 0.17, and 2.3 J/cm^2, all recorded with a larger ∼25 μm diameter fs-LD beam and a delay of 25 μs between desorption and photoionization laser pulses. The threshold fs-LD energy for formation of ion signal was ∼0.08 J/cm^2 (data not shown).

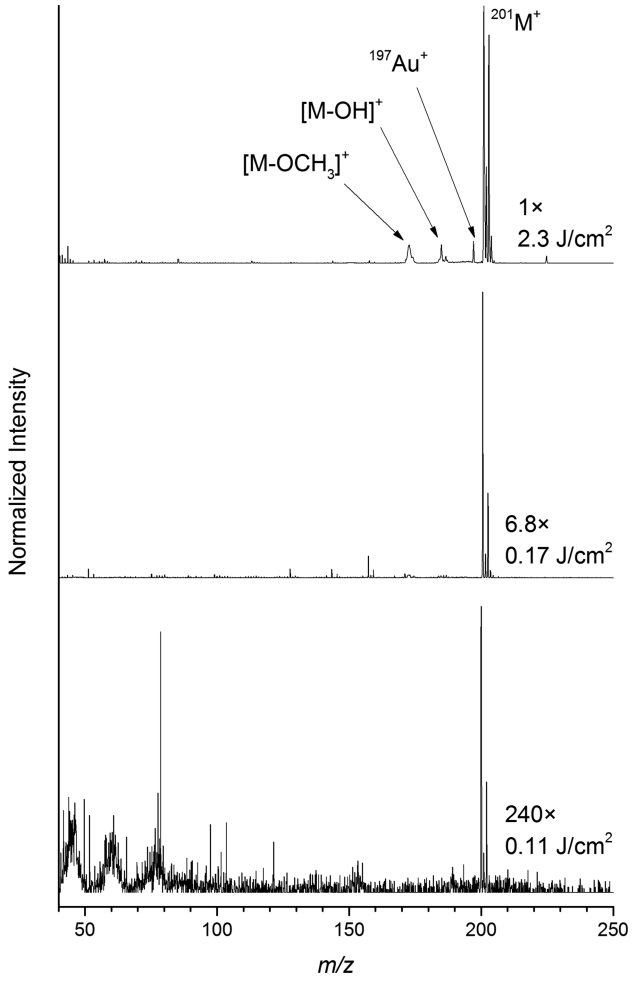

Figure 2. fs-LDPI-MS of 2-methoxy-4-amino-5-chlorobenzoic acid adsorbed onto a 10 layer chitosan/alginate polyelectrolyte multilayer on a Au-coated Si wafer. Spectra recorded at fs-LD fluences of 0.11, 0.17, and 2.3 J/cm^2, all with a fs-LD to postionization laser pulse time delay of 25 μs.

Only the intact precursor ion at m/z 201 was observed for this chlorobenzoic acid ion at a fs-LD pulse energy of 0.11 J/cm^2, with the expected 3:1 ratio of $^{35}Cl/^{37}Cl$ isotopes for m/z 201:203. Almost no fragmentation was observed at 0.11 and 0.17 J/cm^2, but the latter shows ∼35× higher signal. However, higher precursor signal was observed at fs-LD fluence of 2.3 J/cm^2 but at the cost of the additional appearance of fragments at m/z 184 attributed to $[M-OH]^+$ and m/z 170 attributed to $[M-OCH_3]^+$. Furthermore, the appearance of the Au^+ atomic ion at the highest laser fluence of 2.3 J/cm^2 indicates that the entire multilayer was disrupted by the fs-LD event. It should be noted that the spectra in Figure 2 represent the sum of at least 50 individual mass spectra recorded from separate spots on the sample.

Figure 3 shows the fs-LDPI-MS of 2-methoxy-4-amino-5-chlorobenzoic acid on the multilayer at 5, 25, and 99 μs delay between firing of the two lasers, at a fixed fs-LD pulse energy of 0.17 J/cm^2 and with the same larger fs-LD beam (and also summing 50 spectra). While strong precursor ion signal was observed for all three delays, molecular fragmentation decreased as delay increased. Essentially, no fragmentation was observed at the longest delay of 99 μs, albeit at a significant reduction in detectable ion signal, and maximum signal was

dx.doi.org/10.1021/ac5041154 | Anal. Chem. 2015, 87, 367−371

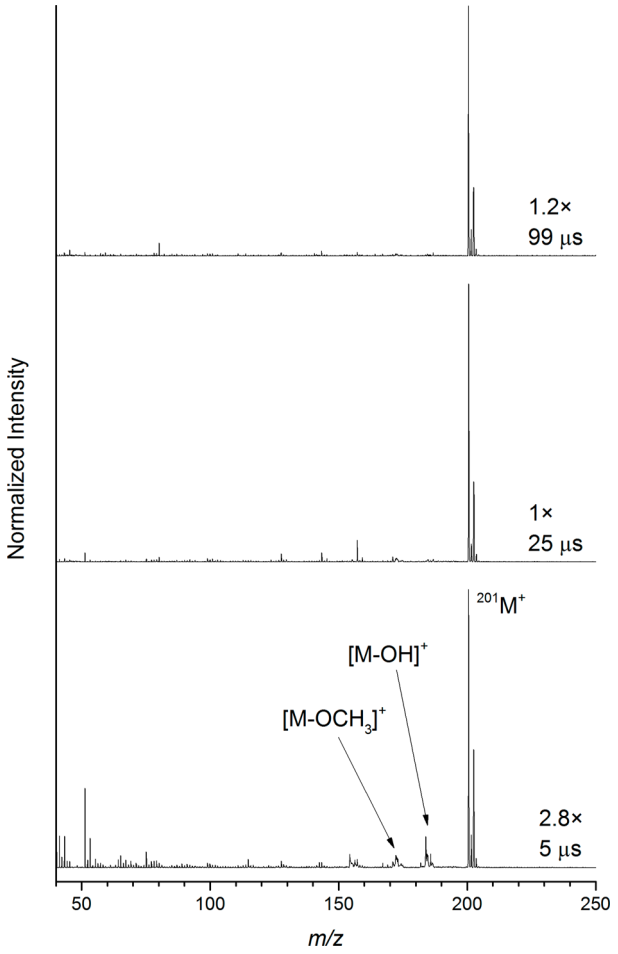

Figure 3. fs-LDPI-MS of 2-methoxy-4-amino-5-chlorobenzoic acid on multilayer, all recorded at fs-LD fluence of 0.17 J/cm^2 and fs-LD to postionization time delays of 5, 25, and 99 μs.

observed here at ~25 μs. It was recently reported that 20−40 μs delays presented the optimal balance between maximizing signal and minimizing fragmentation in fs-LDPI for both these multilayers and bovine eye tissue.[17] These results indicate that variation of the desorption to postionization delay can be used to fine-tune fragmentation, facilitating compound identification in a fashion similar to that employed via postsource decay in MALDI and other time-of-flight MS experiments.

CONCLUSIONS

The use of ultrashort near-IR laser pulses for desorption in conjunction with VUV laser postionization imparts a unique synergy which yields fundamental advantages for MS imaging of a simulated electronic device and should be applicable to biomedical samples. First, the increased number of detectable ions in a single laser desorption event enabled by laser postionization of desorbed neutrals permits using lower fs-LD irradiance so that the effective size of the laser microprobe can be made considerably smaller than the actual diameter of the desorbing laser beam spot, thanks to a highly nonlinear, multiphoton ionization-induced ablation process. Second, the use of lower laser desorption irradiances results in noticeably reduced molecular fragmentation,[17] which can become virtually undetectable under certain combinations of desorption and postionization conditions. Furthermore, the damage to the remaining undesorbed target material is minimized under such conditions, facilitating accurate depth profiling[25,35] and thus three-dimensional MS imaging. Third, the variation of the time delay between desorbing and postionizing laser pulses offers an efficient tool to control and fine-tune the molecular fragmentation, which can help improve accuracy of the molecular species identification.

Prior work showed that useful molecular ion signal can be generated by fs-LDPI without introduction of the matrix compounds, nanoparticles, metal additives, or nanostructures required by other LD-based MS imaging methods.[16,17] When considered in light of the universal nature of ultrashort pulse laser desorption[19,26−31] and the ability of VUV single photon ionization to detect a wide range of molecular and atomic species,[32] it is clear that fs-LDPI-MS will be effective for the near-surface analysis of a wide range of inorganic, organic, synthetic, and biological solids. The experiments presented here demonstrate <2 μm lateral resolution for fs-LDPI-MS imaging, which in many cases should permit single cell imaging. Efforts are currently underway to advance this resolution to the submicrometer level by further improving the instrument sensitivity (so that measurements at even lower desorbing laser irradiances can be conducted) and by reducing mechanical vibrations. However, the high surface roughnesses typical of many biological samples will induce the objective-focused laser beam (with its small, ~10 μm Rayleigh range) to desorb widely varying amounts of material from pulse to pulse from such rough samples. The determination of the lateral resolution for fs-LDPI-MS imaging must therefore be examined on actual biological samples in conjunction with the collection of additional morphological information.

ASSOCIATED CONTENT

Supporting Information

A more thorough experimental description of the mass spectrometer, knife edge scan results showing the fs laser beam radius and Rayleigh range, a fs-LDPI mass spectrum of pentacene, and a figure demonstrating the principle of high lateral resolution imaging by fs-LD. This material is available free of charge via the Internet at http://pubs.acs.org.

AUTHOR INFORMATION

Corresponding Author

*Tel: +1-312-996-0945. E-mail: LHanley@uic.edu.

Notes

The authors declare no competing financial interest.

ACKNOWLEDGMENTS

This work was supported by the U.S. National Science Foundation (DMR-1206175) and the University of Illinois at Chicago.

REFERENCES

(1) Chughtai, K.; Heeren, R. M. A. *Chem. Rev.* **2010**, *110*, 3237−3277.
(2) Watrous, J. D.; Dorrestein, P. C. *Nat. Rev. Microbiol.* **2011**, *9*, 683−694.
(3) Seeley, E. H.; Caprioli, R. M. *Anal. Chem.* **2012**, *84*, 2105−2110.
(4) Vertes, A.; Hitchins, V.; Phillips, K. S. *Anal. Chem.* **2012**, *84*, 3858−3866.
(5) Bhardwaj, C.; Hanley, L. *Nat. Prod. Rep.* **2014**, *31*, 756−767.
(6) Dreisewerd, K. *Anal. Bioanal. Chem.* **2014**, *406*, 2261−2278.
(7) Guenther, S.; Koestler, M.; Schulz, O.; Spengler, B. *Int. J. Mass Spectrom.* **2010**, *294*, 7−15.

(8) Zavalin, A.; Yang, J.; Haase, A.; Holle, A.; Caprioli, R. *J. Am. Soc. Mass Spectrom.* **2014**, *25*, 1079−1082.
(9) Soltwisch, J.; Göritz, G.; Jungmann, J. H.; Kiss, A.; Smith, D. F.; Ellis, S. R.; Heeren, R. M. A. *Anal. Chem.* **2014**, *86*, 321−325.
(10) Zavalin, A.; Todd, E. M.; Rawhouser, P. D.; Yang, J.; Norris, J. L.; Caprioli, R. M. *J. Mass Spectrom.* **2012**, *47*, 1473−1481.
(11) Schmitz, T. A.; Gamez, G.; Setz, P. D.; Zhu, L.; Zenobi, R. *Anal. Chem.* **2008**, *80*, 6537−6544.
(12) Lanni, E.; Dunham, S. B.; Nemes, P.; Rubakhin, S.; Sweedler, J. *J. Am. Soc. Mass Spectrom.* **2014**, *25*, 1897−1907.
(13) Trouillon, R.; Passarelli, M. K.; Wang, J.; Kurczy, M. E.; Ewing, A. G. *Anal. Chem.* **2012**, *85*, 522−542.
(14) Gilmore, I. S. *J. Vac. Sci. Technol., A* **2013**, *31*, 050819.
(15) Coello, Y.; Jones, A. D.; Gunaratne, T. C.; Dantus, M. *Anal. Chem.* **2010**, *82*, 2753−2758.
(16) Cui, Y.; Bhardwaj, C.; Milasinovic, S.; Carlson, R. P.; Gordon, R. J.; Hanley, L. *ACS Appl. Mater. Interface* **2013**, *5*, 9269−9275.
(17) Milasinovic, S.; Cui, Y.; Gordon, R. J.; Hanley, L. *J. Phys. Chem. C* **2014**, DOI: 10.1021/jp504062u.
(18) Flanigan, P. M.; Shi, F.; Perez, J.; Karki, S.; Pfeiffer, C.; Schafmeister, C.; Levis, R. J. *J. Am. Soc. Mass Spectrom.* **2014**, *25*, 1572−1582.
(19) Maxwell, S.; Mazur, E. *Med. Laser Appl.* **2005**, *20*, 193−200.
(20) Cui, Y.; Moore, J. F.; Milasinovic, S.; Liu, Y.; Gordon, R. J.; Hanley, L. *Rev. Sci. Instrum.* **2012**, *83*, 093702.
(21) Gao, Y.; Lin, Y.; Zhang, B.; Zou, D.; He, M.; Dong, B.; Hang, W.; Huang, B. *Anal. Chem.* **2013**, *85*, 4268−4272.
(22) Blaze M. T., M.; Takahashi, L. K.; Zhou, J.; Ahmed, M.; Gasper, G. L.; Pleticha, F. D.; Hanley, L. *Anal. Chem.* **2011**, *83*, 4962−4969.
(23) Bhardwaj, C.; Moore, J. F.; Cui, Y.; Gasper, G. L.; Bernstein, H. C.; Carlson, R. P.; Hanley, L. *Anal. Bioanal. Chem.* **2013**, *405*, 6969−6977.
(24) Sato, M. Resolution. In *Handbook of Charged Particle Optics*, second ed.; Orloff, J., Ed.; CRC Press: Boca Raton, 2009; pp 392−435.
(25) Milasinovic, S.; Liu, Y.; Bhardwaj, C.; Blaze M. T., M.; Gordon, R. J.; Hanley, L. *Anal. Chem.* **2012**, *84*, 3945−3951.
(26) Krüger, J.; Kautek, W. Ultrashort pulse laser interaction with dielectrics and polymers. In *Polymers and Light*; Springer: New York, 2004; pp 247−290.
(27) Bonse, J.; Baudach, S.; Krüger, J.; Kautek, W.; Lenzner, M. *Appl. Phys. A: Mater. Sci. Process.* **2002**, *74*, 19−25.
(28) Pronko, P.; Dutta, S.; Squier, J.; Rudd, J.; Du, D.; Mourou, G. *Opt. Commun.* **1995**, *114*, 106−110.
(29) Kuper, S.; Stuke, M. *Appl. Phys. Lett.* **1989**, *54*, 4−6.
(30) Konig, K.; Riemann, I.; Fritzsche, W. *Opt. Lett.* **2001**, *26*, 819−821.
(31) Mercadier, L.; Rayner, D. M.; Corkum, P. B. *Phys. Rev. Appl.* **2014**, *2*, 034001.
(32) Hanley, L.; Zimmermann, R. *Anal. Chem.* **2009**, *81*, 4174−4182.
(33) Kostko, O.; Takahashi, L. K.; Ahmed, M. *Chem., Asian J.* **2011**, *6*, 3066−3076.
(34) Vogel, A.; Venugopalan, V. *Chem. Rev.* **2003**, *103*, 577−644.
(35) Milasinovic, S.; Liu, Y.; Gasper, G. L.; Zhao, Y.; Johnston, J. L.; Gordon, R. J.; Hanley, L. *J. Vac. Sci. Technol., A* **2010**, *28*, 647−651.